












RESEARCH ARTICLE

Alteration of the tree–soil microbial system triggers a feedback loop that boosts holm oak decline

Manuel Encinas-Valero¹  | Raquel Esteban²  | Ana-Maria Hereş^{1,3}  | María Vivas⁴  |
Alejandro Solla⁴  | Gerardo Moreno⁴  | Tamara Corcobado⁵  | Iñaki Odriozola⁶  |
Carlos Garbisu⁷  | Lur Epelde⁷  | Jorge Curiel Yuste^{1,8} 

¹BC3-Basque Centre for Climate Change, Scientific Campus of the University of the Basque Country, Leioa, Bizkaia, Spain; ²Department of Plant Biology and Ecology, University of Basque Country (UPV/EHU), Leioa, Bizkaia, Spain; ³Faculty of Silviculture and Forest Engineering, Transilvania University of Braşov, Braşov, Romania; ⁴Faculty of Forestry, Institute for Dehesa Research (INDEHESA), Universidad de Extremadura, Plasencia, Spain; ⁵Department of Forest Protection and Wildlife Management, Phytophthora Research Centre, Faculty of Forestry and Wood Technology, Mendel University in Brno, Brno, Czech Republic; ⁶Institute of Microbiology of the Czech Academy of Sciences, Prague, Czech Republic; ⁷Department of Conservation of Natural Resources, NEIKER-Basque Institute for Agricultural Research and Development, Basque Research and Technology Alliance (BRTA) Parque Científico y Tecnológico de Bizkaia, Derio, Spain and ⁸IKERBASQUE, Basque Foundation for Science, Bilbao, Bizkaia, Spain

Correspondence

Manuel Encinas-Valero

Email: mencinas005@ikasle.ehu.eus

Funding information

Spanish Government Iberyca, Grant/Award Number: CGL201784723P; Spanish Government Jun de la Cierva, Grant/Award Number: IJCI 2017 34640; Spanish Government Mara de Maeztu, Grant/Award Number: MDM 2017 0714; Spanish Government SMARthealth, Grant/Award Number: PID2020113244GA22; Spanish Government SMARTSOIL, Grant/Award Number: PID2020113244GBC21

Handling Editor: Mark Tjoelker

Abstract

1. In anthropic savanna ecosystems from the Iberian Peninsula (i.e. dehesa), complex interactions between climate change, pathogen outbreaks and human land use are presumed to be behind the observed increase in holm oak decline. These environmental disturbances alter the plant–soil microbial continuum, which can destabilize the ecological balance that sustains tree health. Yet, little is known about the underlying mechanisms, particularly the directions and nature of the causal–effect relationships between plants and soil microbial communities.
2. In this study, we aimed to determine the role of plant–soil feedbacks in climate-induced holm oak decline in the Iberian dehesa. Using a gradient of holm oak health, we reconstructed key soil biogeochemical cycles mediated by soil microbial communities. We used quantitative microbial element cycling (QMEC), a functional gene-array-based high-throughput technique to assess microbial functional potential in carbon, nitrogen, phosphorus and sulphur cycling.
3. The onset of holm oak decline was positively related to the increase in relative abundance of soil microbial functional genes associated with denitrification and phosphorus mineralization (i.e. *nirS3*, *ppx* and *pqqC*; parameter value: 0.21, 0.23 and 0.4; $p < 0.05$). Structural equation model ($\chi^2 = 32.26$, $p\text{-value} = 0.73$), moreover, showed a negative association between these functional genes and soil nutrient availability (i.e. mainly mineral nitrogen and phosphate). Particularly, the holm oak crown health was mainly determined by the abundance of phosphate (parameter value = 0.27; $p\text{-value} < 0.05$) and organic phosphorus (parameter value = -0.37; $p\text{-value} < 0.5$).

This is an open access article under the terms of the [Creative Commons Attribution-NonCommercial-NoDerivs](https://creativecommons.org/licenses/by-nc-nd/4.0/) License, which permits use and distribution in any medium, provided the original work is properly cited, the use is non-commercial and no modifications or adaptations are made.

© 2023 The Authors. *Functional Ecology* published by John Wiley & Sons Ltd on behalf of British Ecological Society.

4. Hence, we propose a potential tree–soil feedback loop, in which the decline of holm oak promotes changes in the soil environment that triggers changes in key microbial-mediated metabolic pathways related to the net loss of soil nitrogen and phosphorus mineral forms. The shortage of essential nutrients, in turn, affects the ability of the trees to withstand the environmental stressors to which they are exposed.

KEYWORDS

biogeochemical cycles, defoliation, dehesa, *Quercus ilex*, soil functional genes, soil microbial communities

1 | INTRODUCTION

Plant–soil feedbacks are established when plants alter soil conditions that affect the plant component. This phenomenon operates through several pathways in which changes in plant physiology and metabolism may induce alterations in the composition and activity of the soil biota (i.e. microbial community structure, soil fauna), as well as biochemical and chemical soil properties and processes (i.e. biogeochemical cycles or nutrient availability). This ultimately affects plant performance (Ehrenfeld et al., 2005). One significant factor contributing to these modifications in soil biotic, chemical and biochemical component is the alteration in the supply of plant exudates or litter to the soil (Curiel Yuste et al., 2007, 2010). In the same way, soil also affects plant health. For instance, microbial metabolism is the great engine of carbon and nutrient cycling contributing to the availability of soil nutrients (Willey et al., 2008). Overall, alterations of these mechanisms at the soil level may exert positive or negative effects on plant growth and fitness (Bezemer et al., 2020) and hence on species composition and ecosystem functioning (Png et al., 2023). Disentangling the individual contribution of the different processes involved in these plant–soil feedback and its responses to natural and anthropogenic disturbances associated with climate change (van der Putten et al., 2016) may further facilitate the implementation of effective climate-adaptive forest management (Refsland et al., 2023).

Soil microbial communities play a pivotal role in plant–soil feedbacks through the biogeochemical cycles. Microbial communities are responsible for transforming different forms of carbon, nitrogen, phosphorus and sulphur through a series of redox reactions that change the properties and the availability of the essential soil nutrients (Willey et al., 2008). The contribution of the soil microbial communities to nutrient cycling lies on their metabolic diversity and their capacity to use different molecules as energy sources and electron acceptors. Thus, important soil biogeochemical cycles, such as the one of carbon and nitrogen are driven by the balance between the fixation of a gas form (CO_2 , N_2), their incorporation into organic matter and their mineralization and respiration (Singh et al., 2020). In contrast, phosphorus cycling has no gas phase and its assimilation into biological processes exclusively derives from weathering of the phosphate-containing

rocks, the action of phosphate-solubilizing microorganisms or the mineralization and recycling of the organic phosphorus. This fact makes phosphorus unavailability a limiting factor for plant growing in many ecosystems (Moreno et al., 2007; Sardans et al., 2004). Overall, these biogeochemical cycles consist of numerous steps, each mediated by soil microbial functional genes (Zheng et al., 2018). For instance, to assess the microbial potential for nitrogen utilization in different ecological contexts, key functional genes involved in the nitrogen cycle have been used. These include among others: *amoA*, *hao* and *narG* (for nitrification; Francis et al., 2005), *nirK/nirS* and *nosZ* (for denitrification; Henry et al., 2006; Wei et al., 2015) and *nifH* (for nitrogen fixation; Rösch & Bothe, 2005). Understanding how the microbial community metabolism shapes soil biogeochemical cycles is of paramount importance to assess the quality of the soil, its state of degradation (Harris & Bedfordshire, 2003; Tu et al., 2014) and its relationship with plant vulnerability to environmental perturbations (Scarlett et al., 2020).

Climate change-related events may affect biogeochemical cycles (Deng et al., 2021). Drought and high temperatures increase microbial physiological stress by reducing water availability and enzymatic activity, affecting the different biogeochemical processes. For example, drought increases microbial CO_2 emissions and reduces the soil organic carbon content and the mineralization rate of nitrogen (Deng et al., 2021) and phosphorus (Margalef et al., 2017). Tree layer counteracts the negative effects of climate change on the microbial community by buffering extreme temperatures and regulating hydrological conditions under its influence (Prescott, 2002). This favours the resilience of the microbial community to warming and drought scenarios (Avila et al., 2019; San-Emeterio et al., 2023). However, drought and heatwave-induced tree decline events affect physicochemical soil properties and microbial communities, modifying their metabolism and survival rates (Avila et al., 2019; Deng et al., 2021). Microbial communities respond to these disturbances through changes in the population at functional and taxonomic levels. For instance, changes in the abundance of microbial nitrifiers have been related to changes in the canopy cover (Ibañez et al., 2021; Shvaleva et al., 2015) and tree girdling (Rasche et al., 2011). Soil microbial community changes driven by tree decline may result in a net loss

of soil nutrients (Avila et al., 2021; García-Angulo, 2020). Hence, although some studies have described the influence of the canopy cover on soil microclimatic conditions, soil microbiome (García-Angulo et al., 2020) and carbon and nutrient cycling (Ibañez et al., 2021; Scarlett et al., 2020) few studies have assessed the influence of the crown health on biogeochemical soil functional genes, soil chemistry and vice versa. A comprehensive functional examination of the microbial community is key to assess biogeochemical cycling and its role in tree–soil feedback in response to climate change-induced tree decline (Deng et al., 2021; Zheng et al., 2018).

This study focuses on the Spanish dehesa, a savanna-like woodland of agrosilvopastoral use presents in the Iberian Peninsula, where Mediterranean holm oak (*Quercus ilex* L. subsp. *ballota* (Desf.) Samp.), are sparsely distributed. Dehesas are among the most endangered ecosystems in the Mediterranean basin (Pulido et al., 2001) due to drought and heatwave-induced tree decline (Gea-Izquierdo et al., 2021), pathogen outbreaks such as *Phytophthora cinnamomi* Rands (Corcobado et al., 2017; Sánchez-Cuesta et al., 2021) and inappropriate human management (Moreno & Pulido, 2009). Previous works demonstrated that early stress markers extracted from leaves (i.e. carotenoids and tocopherols) were associated with the first stages of holm oak decline (Encinas-Valero, Esteban, Hereş, Becerril, et al., 2022). Furthermore, the decline was also determined by an increase in the fine root phenotypic plasticity (Encinas-Valero, Esteban, Heres, Vivas, et al., 2022). The identification of these responses opened up new opportunities to characterize holm oak health at both above–below-ground compartments during the early stages of holm oak decline. In this regard, our aim was to determine how microbial-mediated biogeochemical cycling, represented by soil functional genes relates with tree crown health, particularly at early stages of holm oak decline. Tree health is subjected to a bidirectional process where tree canopy influences microclimatic soil conditions that, in turn, impact the microbial communities responsible for carbon and nutrient cycling (Ibañez et al., 2021; Rodríguez et al., 2019). Considering that a favourable soil nutrient status is crucial for enhancing holm oak resilience against decline (Camilo-Alves et al., 2013; Sánchez-Cuesta et al., 2022; Serrano et al., 2013), our general hypothesis is that the onset of holm oak decline triggers a tree–soil feedback loop. Specifically: (i) the loss of crown health at early stages of holm oak decline would affect the relative abundance of soil microbial functional genes and hence the functioning of soil microbial communities; and (ii) the alteration in the relative abundance of these soil microbial functional genes would regulate the availability of key soil nutrients that will further impact on the holm oak crown health. The elucidation of this bidirectional process can help to identify components of the tree–soil system factors that are contributing

to and exacerbating this feedback loop. Then, these components can be targeted to mitigate potential damaging feedbacks and the onset of holm oak decline.

2 | MATERIALS AND METHODS

2.1 | Sites description and experimental design

Nine holm oak dehesas, located in the central-west Iberian Peninsula, were considered for this research. All these dehesas were selected based on a previous study (Corcobado et al., 2013) where the interaction between drought and *P. cinnamomi* was identified as the main cause of holm oak decline, however, the presence of this pathogen was not detected in this sampling campaign (c.f. Section 2.5). Their mean monthly temperature and total monthly rainfall ranged from 6.9°C and 29.8 mm in January, to 25°C and 10.4 mm in August 2019 (Harris et al., 2020). The pH of the soil ranged from 4.0 to 7.7. The tree layer, characterized by a low density of the tree canopy cover, was dominated by holm oak whereas the understorey vegetation was dominated by grazing pastures. Climatic conditions and land use and managements of the sampling dehesas are illustrated in Figure S1.

Within each of the nine dehesas, two different sites were considered: a healthy site (i.e. characterized by the presence of only healthy holm oaks) and an unhealthy site (i.e. characterized by the coexistence of trees at early stages of holm oak decline; susceptible and declining holm oaks). The health status of the trees (i.e. healthy, susceptible and declining) was assigned after integrating the results obtained on a previous study (Encinas-Valero, Esteban, Hereş, Becerril, et al., 2022; Encinas-Valero, Esteban, Heres, Vivas, et al., 2022). Briefly, healthy trees ($n=54$) were defined as being those growing in the healthy sites, susceptible trees ($n=59$) were defined as being those that had less than 10% of defoliation but high rates of early stress markers (i.e. photoprotective compounds, Table S1) and declining trees ($n=49$) were defined as being those that had more than 10% of defoliation and high rates of early stress markers (Table S1). Thus, a total of 162 holm oak trees were considered for this study (Table 1).

No permissions were required to access each dehesa other than the landowner's consent.

2.2 | Crown health and root system determination

To numerically define the health of each tree, we combined the results of previous studies (above- and below-ground tree compartments; Encinas-Valero, Esteban, Hereş, Becerril, et al., 2022;

TABLE 1 Table of inference.

Scale of inference	Scale at which the factor of interest is applied	Number of replicates at the appropriate scale
Individuals (holm oak trees)	Individuals (holm oak trees) within nine dehesas	Nine dehesas, 18 holm oak trees per dehesa ($n = 162$)

Encinas-Valero, Esteban, Heres, Vivas, et al., 2022) into a principal component analysis (PCA). Specifically, for the above-ground tree components that characterized the crown health (Encinas-Valero, Esteban, Hereş, Becerril, et al., 2022), we considered early stress markers associated with holm oak decline: (i) the photosynthetic performance index (PiAbs), as a proxy of the photosynthetic energy conservation (Strasser et al., 2000), (ii) chlorophylls (Chl a + b, $\mu\text{mol m}^{-2}$), as a proxy of light harvesting regulation and plant acclimation (Esteban et al., 2015), (iii) the violaxanthin cycle pigment pool (VAZ, violaxanthin + zeaxanthin + antheraxanthin, mmol mol Chl^{-1}), as proxy photoprotective compounds through thermal dissipation (García-Plazaola et al., 2017), (iv) total tocopherols (mmol mol Chl^{-1}), as a proxy of antioxidant compounds (Juvany et al., 2013); and (v) the defoliation (%). As for the characterization of the below-ground compartment, we considered: fine root branching, fine root length (cm) and fine root diameter (cm) as proxies of the resource-uptake strategies of holm oak roots (Encinas-Valero, Esteban, Heres, Vivas, et al., 2022). The results of the PCA showed that the first two axes (Figure 1) explained 50.1% of the variance and segregated the below-ground (PC1) and the above-ground (PC2) tree compartments. The

first axis (PC1; hereinafter, fine root system) accounted for 27.5% of the variance and was defined by the root functional traits: the fine root diameter accounted for the highest loading factor (0.61), while the fine root branching accounted for the lowest loading factor (-0.59). This axis was represented in a gradient colour from brown to yellow, that is, from high fine root branching to high fine root diameter and fine root length. The second axis (PC2; hereinafter, crown health) accounted for 22.6% of the variance and was defined by the level of crown defoliation in combination with the leaf functional traits. The photosynthetic performance index (i.e. PiAbs) had the highest loading factor (0.41) and was positively correlated with the chlorophylls, while the total tocopherol pool had the lowest loading factor (-0.46) and was positively correlated with the defoliation and VAZ. The PC2 axis segregated the sampled holm oaks in a continuous gradient depending on the holm oak crown health (Figure 1). The holm oak crown health was represented using a colour gradient from red (i.e. high total tocopherols pool, VAZ and defoliation, characteristics that defined declining holm oaks) to blue (i.e. high chlorophylls and PiAbs, characteristics that defined the healthy holm oaks; Figure 1).

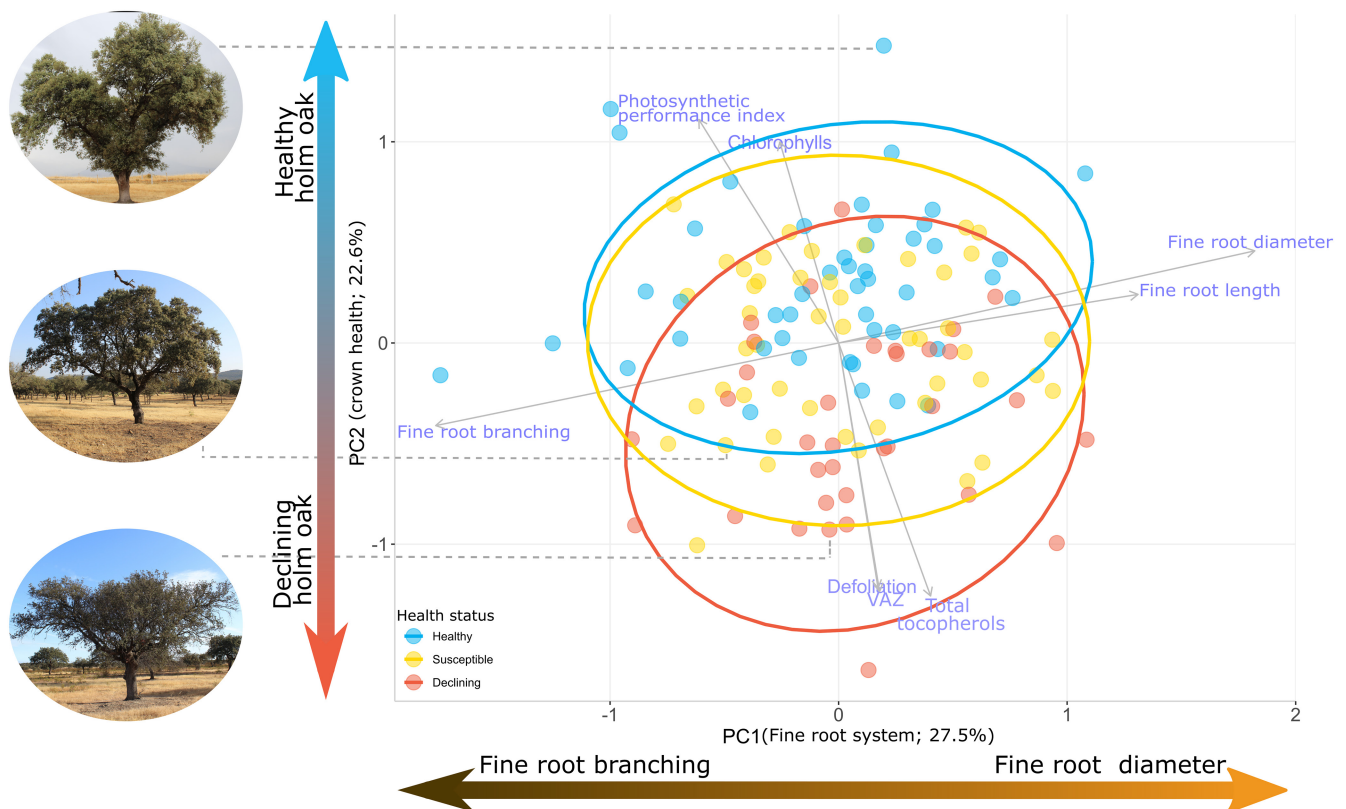


FIGURE 1 Biplot of the principal component analysis showing the first two axes that represent the below-ground (root system) and the above-ground (crown health) tree compartments. The considered below-ground variables were: fine root branching, fine root length (cm) and fine root diameter (cm). The considered above-ground variables were: the photosynthetic performance index, chlorophylls ($\mu\text{mol m}^{-2}$), the violaxanthin cycle pigment pool (i.e. VAZ mmol mol^{-1} Chl), the total tocopherol pool (mmol mol^{-1} Chl) and the defoliation (%). Healthy ($n=47$), susceptible ($n=48$) and declining ($n=34$) holm oak trees are represented in blue, yellow and red respectively. Due to technical problems, some samples were not included in this analysis. Grey arrows indicated the contribution of the analysed variables. The linear combination of the analysed variables (PC1 and PC2) is represented in a colour gradient; from brown to yellow (PC1) and from red to blue (PC2).

2.3 | Soil sampling

To account for the soil spatial heterogeneity, three different soil samples were collected below each of the 162 holm oak trees at a distance of 1 m from each trunk. The depth at which we collected the soil was determined by the depth where the shallowest holm oak fine root density peak was located. As we collected both the soil and the roots at the same depth, and this holm oak root depth was affected by the presence of the herbaceous root layer and historical land management practices (Moreno et al., 2005), we excavated until we reached the soil layer predominantly containing holm oak roots. This typically occurred at an average depth of 15 cm and generally did not exceed 30 cm. Then, the three soil subsamples were pooled in one single composite sample that was maintained at 4°C (12 h) until processing in the laboratory. These soil samples were then used to do soil chemical analyses and to quantify soil microbial functional genes. Specifically, for the soil chemical analyses, the 162 soil samples were dried at room temperature (~20°C), sieved using a 2 mm mesh size and stored in darkness (cf. Section 2.4). Regarding the analysis of soil microbial functional genes, aliquots from the 162 soil samples were frozen at -20°C just upon arrival at the laboratory every day after sampling and stored in darkness for approximately 1 month after sampling, until DNA extraction (cf. Section 2.5).

2.4 | Soil chemical analyses

Total organic carbon content (organic C) was determined using the dichromate oxidation method described by (Yeomans & Bremner, 1988). Total organic nitrogen (organic N) and organic phosphorus (organic P) contents were determined based on the Kjeldahl digestion method (Radojevic et al., 1999). The final results of organic P and N are the sum of organic and inorganic forms although the inorganic part in this determination is considered insignificant compared to the organic part of the soil. All the results were expressed as mg of organic C, N or P per 100 mg of soil (%). The ammonium determination was performed based on the modified Berthelot reaction (Krom, 1980; Searle, 1984), while the nitrate (NO₂⁻) and nitrite (NO₃⁻) contents were determined following the cadmium reduction method (Navone, 1964; Walinga et al., 1989). The mineral N was calculated as the sum of ammonium, nitrite and nitrate. The phosphate soil content was determined following the ammonium heptamolybdate and potassium antimony oxide tartrate reaction in an acidic medium, using a phosphate solution to form the antimony-phospho-molybdate complex (Boltz & Mellon, 1948), while the potassium soil content was determined at 776 nm by aspirating the sample into a flame (Richards, 1954). The ammonium, nitrate, nitrite, phosphate and potassium results were expressed as ppm, µg g⁻¹ of soil. The pH of the soil samples was measured through the saturated soil paste method (Kalra, 1995).

2.5 | Soil microbial functional gene characterization

Soil DNA was extracted from each frozen soil aliquot (250 mg) using the DNAeasy PowerSoil Pro Kit (QIAGEN, Germany) and following the manufacturer's guidelines. Before the extraction, samples were washed twice in 120 mM of K₂PO₄ (pH = 8.0) to remove extracellular DNA (Kowalchuk et al., 2002). The amount of DNA was quantified on a ND-1000 spectrophotometer (Thermo-Scientific, Wilmington, DE).

The abundance, gene copy number relative to 16S, of the soil microbial functional genes, involved in the C, N, P and S cycles, were quantified through high-throughput quantitative PCR (HT-qPCR) by applying the nanofluidic qPCR BioMark™ HD system developed by the Fluidigm Corporation (<https://www.fluidigm.com/>). This system performs qPCR reactions in a Dynamic Array IFC of integrated fluidic circuits and it was applied to the 162 soil DNA samples that corresponded to the 162 studied holm oak trees. A total of 71 validated primer sets (Zheng et al., 2018) were used: 18 targeting C hydrolysis genes (i.e. genes involved in starch, hemicellulose, cellulose, chitin, pectin and lignin degradation); 13 for the C fixation genes; 4 for the methane metabolism (i.e. methane oxidation); 22 for the N cycling (i.e. genes involved in N fixation, nitrification, denitrification, ammonification, anaerobic ammonium oxidation, assimilatory and dissimilatory N reduction and organic N mineralization); 9 for the P cycling genes (i.e. mineralization, solubilization, biosynthesis and hydrolysis of P); and 5 for the S cycling (i.e. S reduction and oxidation). The primer pairs and the encoded enzymes of the analysed soil microbial functional genes may be found in the electronic supplementary material published by (Zheng et al., 2018) and in Table S2. In addition, species-specific primers for the detection of *Phytophthora* spp were used (Table S3). All the samples were pre-amplified through specific Target Amplification STA-reactions with a pool of primers (250 nM) at 14 PCR cycles using the 12.12 FLEXSix Dynamic Arrays IFC and exonuclease I (Thermo Scientific, Cat N. EN0582). These reactions were performed using the GE FLEXSix PCR+Melt v2 protocol. For the amplification, the 1:10 diluted STA reactions were loaded onto the 96.96 Dynamic Array IFC along with the Master Mix SsoFast™ EvaGreen® Supermix with Low ROX (Bio-Rad Laboratories, Redmond, WA), with a final primer concentration, both forward and reverse, of 250 nM. For the thermocycling, an initial denaturation at 95°C was considered for 1 minute. Then, this process was followed by 30 cycles of 5 s at 96°C and 20 s at 60°C followed by a melting curve (from 60°C to 95°C). Three technical replicates per sample were added. The Fluidigm Real-Time PCR Analysis Software (v. 4.1.3.) was used to quantify the cycle threshold (Ct) of the replicates. The Ct cut-off (i.e. detection limit) was established at 29 considering the highest Ct of the technical replicate samples and a standard deviation between replicates below 0.25. The detection of a specific gene in a sample was considered positive when two of three replicates were positive and below the Ct cut-off. The relative abundance of the genes

was expressed as a copy number relative to 16S (Looft et al., 2012; Zheng et al., 2018):

$$GR = 10^{(29-Ct)/(10/3)}$$

$$GR_{\text{per } 16S} = \frac{GR_{\text{target gene}}}{GR_{16S}}$$

where 29 is the detection limit and Ct is the qPCR threshold cycle. Hence, the relative abundance assessed the presence and proportion of specific genes in the microbial community that increased or decreased (Zheng et al., 2018). From the 71 studied genes, 14 were not detected (Figure S2). The relative abundance of a non-detected gene in a sample was considered as being 0.

All the soil microbial functional genes analyses were conducted at the Gene Expression Unit of SGIker (University of the Basque Country UPV/EHU, Spain).

2.6 | Statistical analyses

To estimate the effect of the tree health status (i.e. healthy, susceptible and declining) on the relative abundance of the soil microbial functional genes, a first set of linear mixed effect models (LMEs) were run. The soil microbial functional genes data were transformed (logarithm or square-root) to meet normality and homoscedasticity assumptions and reduce the influence of outliers for model validation. The fixed part of the model included the health status while for the random part of the model, the site (i.e. healthy and unhealthy) was nested within dehesa to account for the among-sampling site variation. All final reported coefficients were estimated based on the restricted maximum likelihood method (REML) and ANOVA Type III (car R package; Fox & Weisberg, 2019) to deal with unbalanced design. Finally, conditional coefficients of determination (i.e. variance explained by the entire model, R^2_c) were calculated using the *r.squaredGLMM* function (Barton, 2020). When significant differences in the health status were found, least-square means tests based on Tukey's HSD were run (Lenth, 2020). Finally, normality and homoscedasticity assumptions of the residuals were checked using the Kolmogorov-Smirnov test, histogram and quantile-quantile plots. To represent the change in the relative abundance of the analysed soil microbial functional genes of the susceptible and declining holm oak trees relative to the healthy holm oak trees (Table S4), the estimated category means and *p*-values were extracted from the post-hoc tests (i.e. least-square means test based on Tukey's HSD). Hence, change relative to healthy trees (CR_H) was calculated as follows:

$$CR_H = \frac{EM_D - EM_H}{EM_H}$$

where EM_D and EM_H are the estimated relative abundances of the analysed genes for the susceptible/declining (EM_D) and healthy (EM_H) trees respectively (Figure 2).

To analyse the relationship between the soil chemical analyses and the different soil microbial functional genes a Spearman

correlation matrix was performed (Figure 3) using the 'rccorr' function from the 'Hmisc' R package (Harrell, 2019).

The multidimensionality of the crown defoliation assessment and the leaf and root functional traits (cf. Section 2.2) was explored by computing principal component analysis (PCA). For this, the *rda* function from the *vegan* package was used (Oksanen et al., 2022). Based on the obtained results (Figure 1) the principal components 1 (PC1; fine root system) and 2 (PC2; crown health) were used for further analyses. PC1 and PC2 axes were represented using a colour gradient (Figure 1) that went from yellow to brown in the case of PC1 (from more root diameter or positive PC1 values to more root branching or negative PC1 values). In the case of PC2, the colour gradient went from blue to red gradient (from healthier holm oaks or positive PC2 values to more declining holm oaks or negative PC2 values).

In order to analyse the influence of the below-ground (PC1; fine root system) and the above-ground (PC2; crown health) tree compartments (cf. Section 2.2) on the soil microbial functional genes (i.e. our first hypothesis), a second set of linear mixed effect models (LMEs) were run. A similar structure with the one explained above was applied but this time using the soil microbial functional genes (i.e. response variable) and PC1/PC2 (i.e. explanatory variable) as fixed factor in the LMEs. The influence of the PC1/PC2 on the analysed soil microbial functional genes (Table S5) is represented in Figure 4. Specifically, the PC1 (fine root system) and PC2 (crown health), increased or decreased the relative abundance of the analysed soil microbial functional genes. These tendencies were represented using the same colour gradient that was used for the PC1 and PC2 (Figure 1) in the cycle step where the gene was involved (Figure 4). Hence, an increase in the relative abundance of a specific gene explained by the fine root branching (i.e. negative values of the PC1 represented from yellow to brown gradient) was represented using the same colour gradient (yellow to brown). Instead, an increase in the relative abundance of a functional gene explained by the loss of crown health (i.e. negative values of the PC2 represented from blue to red gradient) was represented using the same colour gradient (blue to red; Figure 4).

Finally, a structural equation model (SEM) was run to test the potential causal-effect relationships between the loss of crown health (i.e. PC2), the soil microbial functional genes involved in the soil biogeochemical cycles and the soil chemical variables (Figure 5). Briefly, our second hypothesis expected a potential tree-soil feedback through the soil microbial functional genes and chemistry. Specifically, SEM was built based on: (i) the influence of the soil chemistry on the crown health (i.e. PC2); (ii) the influence of the microbial functional genes involved in the inorganic phosphate solubilization, organic P transformation and phosphate transport mechanisms (i.e. *gcd*, *pqqC*, *ppk*, *ppx*, *phnk*, *phoD*, *phoX*) on the soil chemistry that affected the crown health (i.e. phosphate and organic P); (iii) the hypothesis that postulates that phosphorus mineralizing enzymes as phosphatases are directly dependent on mineral nitrogen, defined in the literature (Chen et al., 2020; Margalef et al., 2017) and (iv) the results obtained from our first

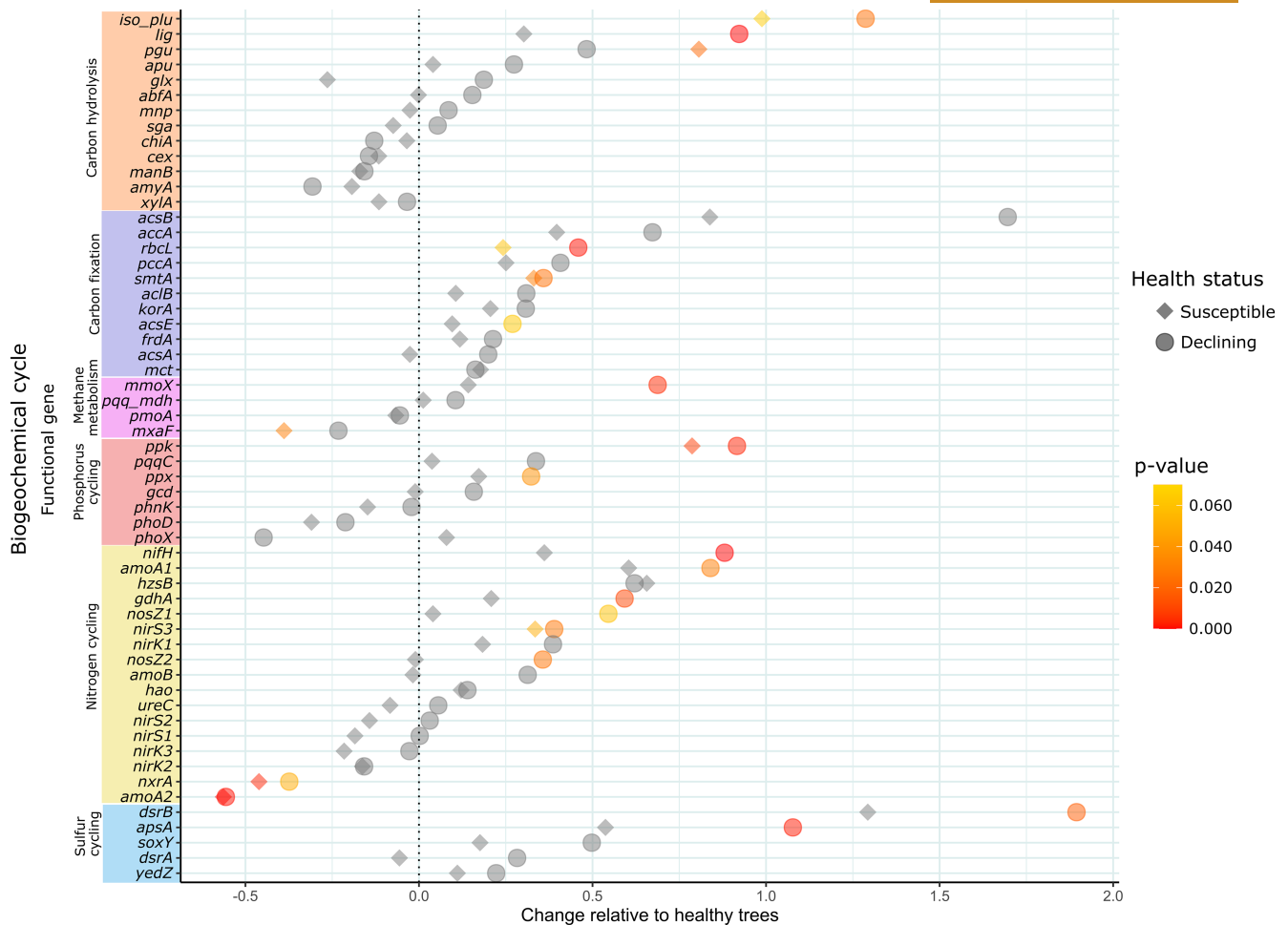


FIGURE 2 Scatter plot showing the changes (relative to the healthy holm oak trees, $n = 54$) in the analysed soil microbial functional genes of the susceptible ($n = 59$) and declining ($n = 48$) holm oak trees. [Table S4](#). Due to technical problems, one sample was not included in this analysis. The analysed microbial functional genes are arranged by their increase relative to healthy trees and by their role in the different biogeochemical cycles: carbon cycling, phosphorus cycling, nitrogen cycling and sulphur cycling. Change relative to healthy trees was calculated using the estimated mean of post-hoc tests from the LMEs for each health status. p -values, extracted from the pairwise differences in health status, are indicated from red (p -value = 0) to yellow (p -value ≤ 0.07).

hypothesis that showed the effect of the crown health (PC2) on the soil microbial functional genes ([Figure 4](#), [Table S5](#)). Thus, in order to meet the first two points (i.e. i and ii) multiple regression models were first performed (i.e. using LMEs and the same random effects explained before). Variables were logarithm or square-root transformed to meet the normality and homoscedasticity assumptions or to reduce the influence of outliers. The best models were selected based on the stepwise AIC (Akaike information criterion) method by using the *stepAIC* function from the MASS package (Venables & Ripley, 2002). To do so, the candidate models were adjusted by the maximum likelihood method (ML). Finally, the results of the best multiple regressions were adjusted by the restricted maximum likelihood method (REML) and the selected explanatory variables were retained for use in SEM. SEM analyses were performed by using the *psem* function available from the *piecwiseSEM* package (Lefcheck, 2016). Several SEMs were run and the best was selected based on Fisher's C statistic (Lefcheck, 2016).

All statistical analyses were performed in R (R Core Team, 2020).

3 | RESULTS

3.1 | Soil nutrient differences among holm oak health status

Briefly, mineral N, nitrate, ammonium, phosphate, potassium and organic C were found to be significantly lower (48%, 65%, 35%, 56%, 37% and 17% respectively) in susceptible and declining trees than in healthy trees ([Figure S3](#)).

3.2 | Phytophthora spp detection

We quantified the relative abundance of each *P. cinnamomi*, *P. quercina* and *Phytophthora* spp. taxon *ballota* relative to oomycete

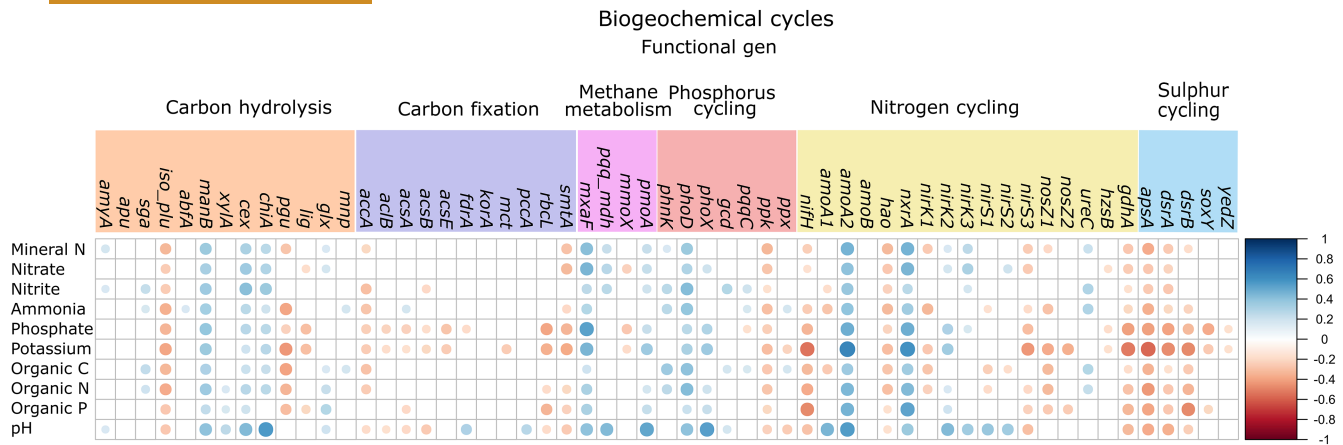


FIGURE 3 Spearman's rank correlation matrix plot depicting the relationships between: (i) soil chemical analysis variables such as mineral N, nitrate, nitrite, ammonia, phosphate, potassium, organic C, organic N and organic P; and (ii) various microbial functional genes associated with biogeochemical cycles, including carbon cycling, phosphorus cycling, nitrogen cycling and sulphur cycling. Negative and positive correlations are represented in red and blue respectively. The strength of the correlations is denoted by dot size.

abundance (Table S3). *Phytophthora cinnamomi* was detected in only four samples (i.e. 84, 85, 125 and 129). *P. quercina* and *Phytophthora* spp. taxon *ballota* were detected in higher proportions, although without a relationship with the health status of the trees (*P. quercina*, $R^2_c = 0.36$; p -value > 0.1 ; *Phytophthora* spp. taxon *ballota*, $R^2_c = 0.16$; p -value > 0.1).

3.3 | Soil microbial functional gene differences among holm oak health status

The relative abundance of the genes involved in the carbon hydrolysis (iso-pullulanase, *iso-plu* and lignin peroxidase, *lig*) were significantly higher in declining (*iso-plu*, 0.008 ± 0.003 ; *lig*, 0.225 ± 0.029) than in healthy trees (*iso-plu*, 0.003 ± 0.0007 ; *lig*, 0.225 ± 0.029 , Figure 2, Table S4). The relative gene abundance for carbon fixation (i.e. ribulose-bisphosphate carboxylase, *rbcl* and S-malate-CoA transferase, *smtA*) was higher in declining trees (*rbcl*, 188.01 ± 17.36 ; *smtA*, 2.398 ± 0.200) than in the healthy trees (*rbcl*, 133.64 ± 10.16 ; *smtA*, 1.8027 ± 0.136 , Figure 2, Table S4). The relative abundances of methane monooxygenase component α chain, *mmoX*; polyphosphate kinase, *ppk* and exopolyphosphatase, *ppx* genes were higher in declining (*mmoX*, 0.530 ± 0.089 ; *ppk*, 0.005 ± 0.0007 ; *ppx*, 2.498 ± 0.182) than in healthy trees (*mmoX*, 0.329 ± 0.050 ; *ppk*, 0.003 ± 0.0003 ; *ppx*, 2.047 ± 0.193 , Figure 2, Table S4). In addition, the relative abundance of alkaline phosphatase/Pho regulon, *phoX* was marginally

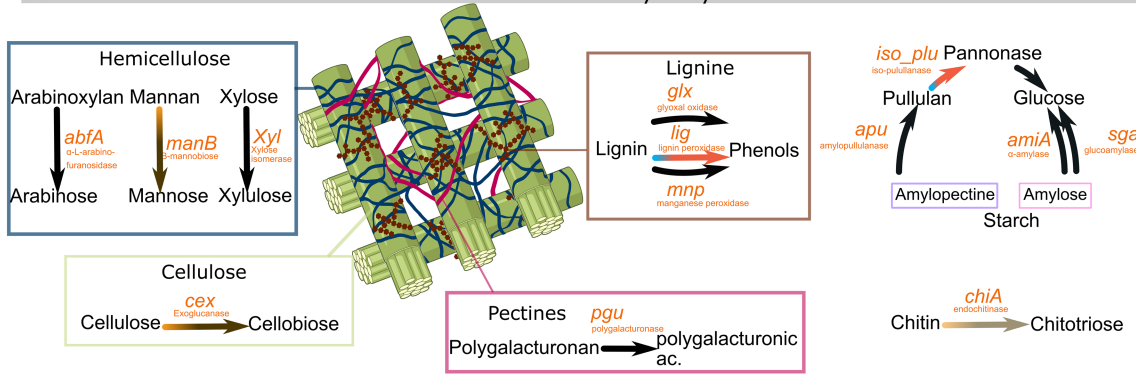
higher ($p = 0.06$) in susceptible (0.098 ± 0.025) than in declining trees (0.056 ± 0.013 , Table S4). Genes involved in the nitrogen cycle, ammonia monooxygenase α subunit for archaea (*amoA1*) was significantly higher in declining trees (233.067 ± 37.03) than in healthy one (139.12 ± 24.129 , Figure 2, Table S4). In contrast, ammonia monooxygenase α subunit for bacteria (*amoA2*) was significantly higher (55%) in healthy trees (3.05 ± 0.48) than in declining trees (1.72 ± 0.42). Nitrogenase iron protein (*nifH*); glutamate dehydrogenase (*gdhA*), nitrous-oxide reductase (*nosZ1/2*) and nitrite reductase (*nirS3*) were significantly more abundant in declining (*nifH*, 31.01 ± 5.51 ; *gdhA*, 80.94 ± 11.02 ; *nosZ2*, 5.52 ± 0.62 ; *nirS3*, 0.43 ± 0.02) than in healthy trees (*nifH*, 19.71 ± 4.44 ; *gdhA*, 55.35 ± 6.52 ; *nosZ2*, 4.39 ± 0.41 ; *nirS3*, 0.35 ± 0.03 , Table S4). Finally, nitrite oxidoreductase α subunit (*nrxA*) was significantly higher ($p < 0.01$) in the healthy (6.31 ± 1.19) trees than in susceptible (3.11 ± 0.58) and declining trees (4.05 ± 0.69 , Figure 2, Table S4). Genes involved in the sulphur cycle (sulphite reductase β subunit, *dsrB* and adenosine-5'-phosphosulfate reductase α subunit, *apsA*) were significantly higher in declining (*dsrB*, 0.74 ± 0.24 ; *apsA*, 0.39 ± 0.13) than in healthy trees (*dsrB*, 0.30 ± 0.07 ; *apsA*, 0.16 ± 0.04).

3.4 | Relationship between soil microbial functional genes and soil chemical analysis

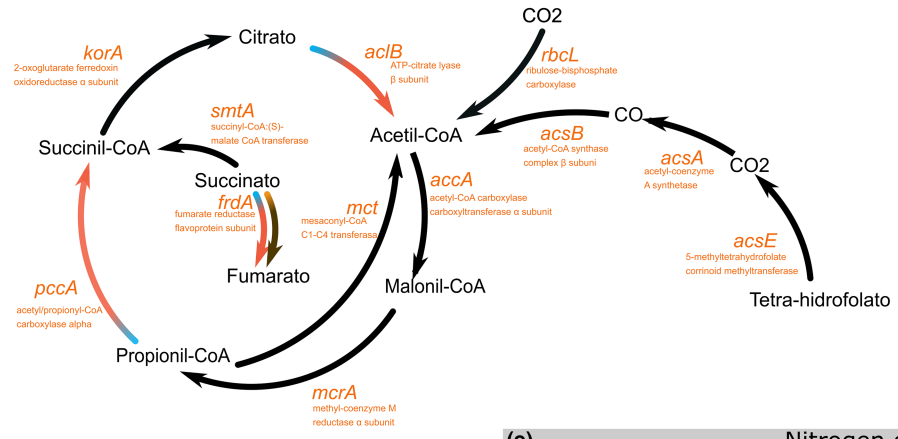
Overall, the genes that showed a higher relative abundance in the unhealthy than in the healthy sites (*iso-plu*, *pgu*, *lig*, *rbcl*,

FIGURE 4 Depiction of the second set of LMEs (Table S5). This figure shows how the different soil microbial functional genes, significantly increased ($p < 0.05$) as a function of the below-ground (fine root system) and above-ground (crown health) tree compartments (Figure 1) in each of the biogeochemical steps where they are involved in carbon hydrolysis (a), carbon fixation (b), methane metabolism (c), phosphorus cycling (d), nitrogen cycling (e) and sulphur cycling (f). This relationship is indicated by the used gradient colour that represents PC1/PC2 in Figure 1. Mild-coloured arrows indicated a marginally significant effect of the principal component (PC1/PC2) on the soil microbial functional genes ($p \leq 0.07$). Instead, the black arrows indicated non-significant effects of the principal components on the analysed soil microbial functional genes. The non-detected genes are not shown. The representation of the biogeochemical cycles is based on the figures published in Zheng et al. (2018).

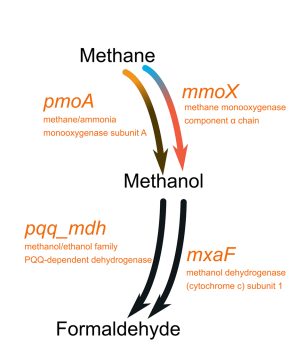
(a) Carbon hydrolysis



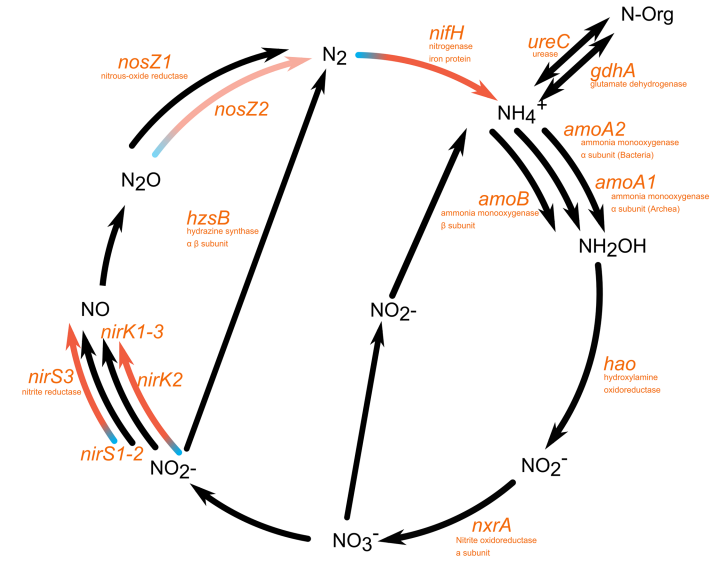
(b) Carbon fixation



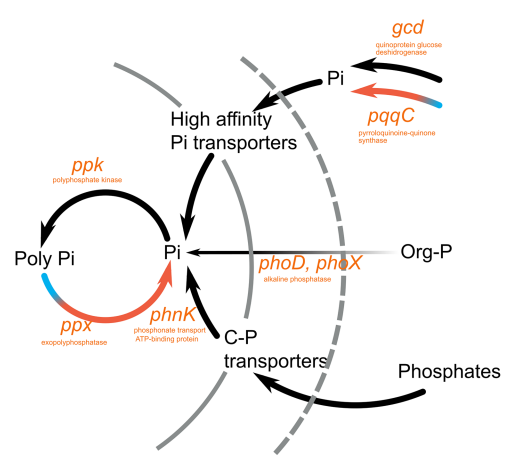
(c) Methane metabolism



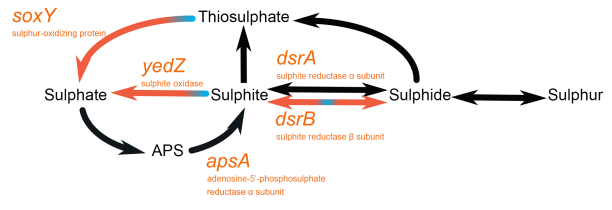
(e) Nitrogen cycling



(d) Phosphorus cycling



(f) Sulphur cycling



Legend for effect significance:

- Black arrow: Non-significant effect of the PC1/PC2
- Red arrow: Significant effect of the PC1/PC2
- Blue arrow: Marginally significant effect of the PC1/PC2

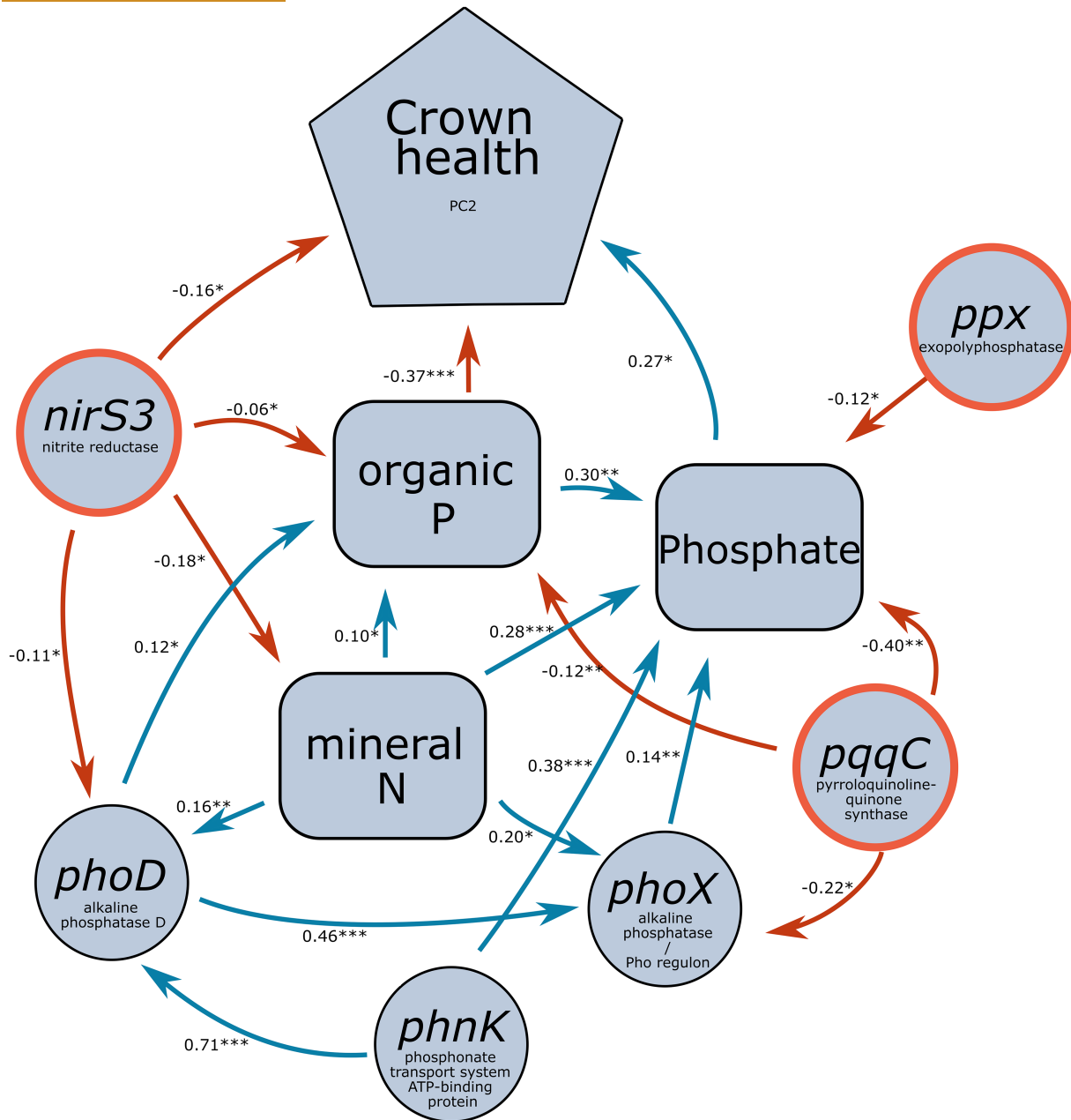


FIGURE 5 Structural equation modelling (SEM) results. The path diagram shows a putative causal–effect relationship among soil functional genes involved in the nitrogen (*nirS3*) and phosphorus cycling (*phoX*, *phoD*, *pqqC*, *ppx*, *phnK*), the mineral N ($\mu\text{g g}^{-1}$), phosphate ($\mu\text{g g}^{-1}$), organic P (%) and crown health (PC2). Arrows indicate causal relationships, numbers indicate the standardized estimated regressions' weights and asterisks represent significant relationships (* $p < 0.05$; ** $p < 0.01$; *** $p < 0.001$). Blue arrows indicate positive relationships while red arrows indicate negative relationships.

smtA, *mmoX*, *ppk*, *ppx*, *nifH*, *amoA1*, *gdhA*, *nirS3*, *nosZ1*, *nosZ2*, *dsrB* and *apsA*) were negatively correlated with the abundance of the different chemical forms of the different nutrients ($\rho < 0$, p -value < 0.05 ; Figure 3). In contrast, the genes that showed a higher relative abundance in the healthy than in the unhealthy sites (*nxrA*, *amoA2* and *mxnF*) were positively correlated with the abundance of the different chemical forms of the different nutrients analysed (Figure 3).

3.5 | Influence of the below-ground and above-ground tree compartments on the microbial community

Figure 4 depicted how the different analysed soil microbial functional genes (relative abundance) significantly increased as a function of the fine root system (PC1) and crown health (PC2) (Figure 4) in each of the biogeochemical steps where they were involved. This was

assessed by the second sets of LMEs (Table S5, Figure 4). A decrease in PC1 led to an increase in the genes involved in mannan and cellulose hydrolysis (β -mannanase, *manB* and exoglucanase, *cex*, Table S5, Figure 4a), as well as, fumarate reductase flavoprotein subunit, *frdA* (Figure 4b). Similarly, PC1 decrease significantly increased the methane/ammonia monooxygenase subunit A, *pmoA*, gene involved in the methane oxidation (Table S5, Figure 4c).

Regarding the influence of the crown health (PC2) on the soil microbial functional genes (Table S5, Figure 4), the genes involved in lignin (*lig*) and starch hydrolysis (*iso-plu*) significantly increased, while PC2 (crown health) decreased, (Table S5, Figure 4a). Fumarate reductase flavoprotein subunit (*frdA*), ATP-citrate lyase β subunit (*aclB*), the acetylpropionyl-CoA carboxylase (*pccA*) and the methane monooxygenase (*mmoX*) also increased, while PC2 decreased (Table S5, Figure 4b,c). In addition, the genes that were involved in the denitrification were also affected by the loss of crown health (PC2). Specifically, copper and haem-containing nitrite reductase (*nirK1* and *nirS3* respectively) significantly increased, while PC2 decreased (Table S5, Figure 4e). In the same way, the genes that were involved in the reduction of the nitrous oxide to nitrogen gas, were found to marginally increased, while PC2 decreased (*nosZ2*, p -value=0.064). The gene involved in the nitrogen fixation (*nifH*) significantly increased, while PC2 decreased. With regard to the phosphorus cycling, the genes that codified the pyrroloquinoline-quinone synthase (*pqqC*) and the exopolyphosphatase (*ppx*) significantly increased, while PC2 decreased (Table S5, Figure 4d). Finally, the genes associated with sulphur oxidation, including sulphur-oxidizing protein (*soxY*), sulphur oxidase (*yedZ*) and sulphite reductase β subunit (*dsrB*), showed a significant increase, while PC2 decreased (Table S5, Figure 4f).

3.6 | Holm oak decline triggered a feedback loop

Figure 5 illustrated hypothesized causal-effect relationships among the components involved in the feedback process triggered by holm oak decline. It also showed how alterations in the relative abundance of soil microbial functional genes regulated the availability of key soil nutrients, subsequently impacting holm oak crown health. (hypothesis 2). Particularly, Figure 5 described the following interconnected processes: (i) the loss of crown health led to an increase in soil functional genes associated with nitrogen and phosphorus cycling (*nirS3*, *ppx* and *pqqC*; marked by red circles), (ii) abundances of these soil functional genes, in turn, affected the availability of min. N, phosphate, and organic P in the soil, (iii) changes in soil nutrient availability subsequently influenced crown health and (iv) mineral nitrogen affects *phoD*- and *phoX*-harbouring communities. The proposed SEM provided a good fit as indicated by the Fisher's C statistic and p -value ($\chi^2=32.26$, p -value=0.73). According to the results of this analysis (Figure 5), the phosphorus cycling was proposed to be the key biogeochemical cycle that determined the leaf health of the studied holm oak trees. This influence was mainly based on the negative and positive effects of organic P and phosphate on PC2 (the

crown health) respectively (Figure 5). The soil microbial functional genes involved in the phosphorus cycling (*pqqC* and *ppx*, positively affected by PC2) had a negative effect on the organic P and phosphate concentration. In addition, a plausible relationship between nitrogen and phosphorus cycling through genes that codified alkaline phosphatases (*phoX* and *phoD*) and the negative effect of the denitrifier communities (*nirS3*, positively affected by PC2) on the mineral N pool was shown (Figure 5).

4 | DISCUSSION

According with our general hypothesis, our study described the reciprocal relationship between the trees and soil in dehesas, encompassing critical aspects of holm oak health (i.e. early stress markers and defoliation triggered by drought and high temperatures) along with the biological (soil functional genes) and chemical (soil nutrients) component of the soil. These relationships were characterized by a feedback loop, in which the result of the process (loss of crown health) favoured the conditions (i.e. net loss of phosphate and mineral N) that favour the onset of holm oak decline. Given that climate change-related events (i.e. drought and heatwaves) are acting as inciting factor for the decline of holm oak (Gea-Izquierdo et al., 2021; Sánchez-Cuesta et al., 2021), and considering the self-exacerbating nature of this feedback (Figure 5), its onset will inevitably result in the death of the tree unless appropriate measures are implemented (Rodríguez-Calcerrada et al., 2017). Below we describe the two directions of causation and the mechanisms involved.

4.1 | The loss of crown health affects the relative abundance of the soil microbial functional genes

Tree decline affects the soil abiotic and biotic environments under its influence (Curiel Yuste et al., 2019; Flores-Rentería et al., 2018; García-Angulo et al., 2020) having both direct (Solla et al., 2021) and indirect (Rodríguez et al., 2016) effects on the soil properties. The overall biological functioning of the soil system is affected (Curiel Yuste et al., 2019). In agreement with our first specific hypothesis, our results indicated that the onset of holm oak decline may potentially influence specific biogeochemical processes including: denitrification, lignin and starch degradation, carbon fixation, inorganic phosphorus solubilization and sulphite oxidation (Figure 4, Table S5). As observed here, changes in the soil abiotic environment, due to a reduction in the tree cover (i.e. increase in temperature and water content, reduction of organic matter and soil nutrients), have been directly associated with alterations in the abundance of nitrogen-transforming microorganisms (i.e. increases in NO_2 associated with increases in *nosZ*; Shvaleva et al., 2015; nitrifiers, García-Angulo et al., 2020; or *amoA*-harbouring communities (Scarlett et al., 2020). In this study, denitrifiers (*nirS3*, *nirK1* and *nosZ2*) and nitrogen fixation communities (*nifH*) were enhanced by the initial loss of crown health (Table S5, Figure 4). This contrasting result may

be partly explained by the polyphyletic distribution of denitrifying genes and their co-occurrence with nitrogen fixation genes in many strains (Levy-Booth et al., 2014). In addition, *nirS3*- and *nirK1*-harbouring communities were negatively correlated with the availability of mineral N, nitrate and ammonia (Figure 3). This suggested that these communities may be implicated in the loss of mineral nitrogen through denitrification. This phenomenon constitutes a net potential source of nitric oxide (NO) that could explain the depletion of mineral N under declining trees. In addition, full denitrification (i.e. N_2O reduction to N_2 by *nosZ*-harbouring communities) may be enhanced by the increase in soil water content as a result of the loss of tree cover (Ibañez et al., 2021; Rasche et al., 2011; Shvaleva et al., 2015) or tree decline (Corcobado et al., 2013; Rodríguez et al., 2023), because the loss of leaves, the stomatal closure and the inability of the tree to uptake soil water due to the pathogen root rot reduce evapotranspiration.

Concerning the rest of the affected biogeochemical cycles, this study also reported the presence of higher values of starch and lignin-degrading genes (*iso-plu* and *lig*, Figure 4, Table S5) associated with the loss of crown health and early declining symptoms. This may be explained by an increasing presence of saprotrophs, wood degraders and/or tree pathogens, probably involved in the loss and degradation of necrotic fine roots in declining trees (Pinho et al., 2020; Solís-García et al., 2021). Also, the increase in *soxY*-, *yedZ*- and *dsrB*-harbouring communities (Figure 4, Table S5) indicated the presence of sulphur-oxidizing bacteria. Some of these bacteria have also the capacity to use oxidized nitrogen forms as terminal electron acceptors, resulting in denitrification under anaerobic conditions (Willey et al., 2008). Moreover, the increase in genes involved in the reverse tricarboxylic acid cycle (Campbell et al., 2003) in conjunction with 3-hydroxypropionate cycle (*pccA*) indicated an increase in carbon fixation potential. The reduction in soil carbon turnover due to holm oak decline (García-Angulo et al., 2020) may slightly favour microbial carbon fixation as a homeostatic response to the progressive soil carbon depletion (Xiao et al., 2022). In addition, the higher relative abundance of *pqqC*- and *ppx*-harbouring communities also indicated the potential for inorganic P solubilization (Meng et al., 2022; Zheng et al., 2018). Overall, several implications arose from the increase in these functional genes, including their involvement in soil nutrient loss, the increased occurrence of tree-damaging pathogens, the reduction of tree-derived carbohydrate inputs to soil and the increase in competition for soil resources between microbial communities and the tree.

4.2 | Microbial-induced changes in nutrient cycling regulate tree health

According to our second specific hypothesis, the obtained results suggested potential changes in the soil microbial functional genes that may be directly related to changes in soil nutrient cycling (Figure 3), ultimately affecting the availability of soil nutrients (Figure 5), essential for crown health. Soil microbial communities

may support or constrain tree performance under stress through the modulation of soil nutrients (Smith et al., 2015). In this sense, *nirS3*-harbouring communities were enhanced by the loss of crown health and had a negative effect on mineral N (Figure 5). Thus, it is likely that *nirS*-harbouring communities may partly consume nitrogen mineral forms, resulting in nitrogen loss through gas emissions under declining holm oaks. This will further reduce nitrogen availability for plants and other bacterial communities (Lennon & Houlton, 2017). The unavailability of nitrogen has been described to be responsible for the downregulation of phosphorus cycling rates, in the short term (Chen et al., 2020). This is because, under phosphorus limitation, phosphorus mineralizing enzymes as phosphatases are N-rich enzymes directly dependent on mineral nitrogen (Chen et al., 2020; Margalef et al., 2017; Marklein & Houlton, 2012), and its absence promotes the accumulation of organic P and the decrease in phosphates, becoming the limiting factor for holm oak growth (Avila et al., 2016). In agreement with this idea, SEM (Figure 5) described how both mineral N shaped *phoD*- and *phoX*-harbouring communities, responsible for hydrolysing carbon-phosphorus ester bonds to phosphate under phosphorus shortage (Ragot et al., 2017). Hence, the shortage of mineral N might have been responsible, at least partially, for the phosphate depletion observed under declining trees and for the further effect on early stress markers associated with the loss of crown health and early tree decline (PC2, Figure 5). As in previous studies, the obtained results highlighted the role of organic P and phosphate in holm oak health (Avila et al., 2016; Sardans et al., 2004) and indicated that the unavailability of phosphate may have increased early stress markers associated with the loss crown health. In this regard, phosphorus limitation has been reported to reduce holm oak biomass (Sardans et al., 2004) and water use efficiency, resulting in faster leaf senescence (El-Madany et al., 2021). In contrast, organic P abundance showed a negative effect on PC2 (Figure 5) in agreement with a previous study that reported a negative effect in the physiology of leaves in *P. cinnamomi*-infected holm oak when an organic fertilizer at high dose was applied (López-Sánchez et al., 2022).

The results of the SEM further illustrated alternative metabolic paths involving the use and dynamics of inorganic forms of phosphorus directly regulated by microbial communities (i.e. *pqqC* and *ppx*, Figure 5). In the case of *pqqC*- and *ppx*-harbouring communities, responsible for inorganic P mobilization (Bi et al., 2019; Wu et al., 2022), they both increased, while crown health (PC2) decreased (Figures 4 and 5, Table S5). While *ppx* genes encode enzymes involved in bacterial intracellular polyphosphate degradation, *pqqC*-harbouring communities promote the solubilization of the recalcitrant phosphorus-metal complex by producing organic acids (Hwangbo et al., 2003). While it might be presumed that these communities increase the phosphorus availability for the trees (Wu et al., 2022), we observed a negative relationship with the soil phosphate concentrations. In this sense, studies under controlled and field conditions have shown inconsistent effects concerning plant performance and inorganic phosphorus solubilization by microorganisms (Meyer et al., 2019). This is because soil characteristics (i.e.

phosphorus, organic C, nitrogen shortage, pH and soil texture) may affect the functioning and effectiveness of the *pqqC*- and *ppx*-harbouring communities to solubilize available phosphorus for tree uptake (Raymond et al., 2020). Thus, we suggest that these communities might be potential competitors for the available phosphate with the tree (Raymond et al., 2020), since inorganic P solubilization is an energy-demanding metabolic path rather unlikely to increase under the low organic C availability of these soils and at intense competence with other microorganisms (Meyer et al., 2019). In any case, the results of this study pointed out *pqqC*- and *ppx*-harbouring communities as potential key regulators of the phosphorus cycle in dehesa ecosystems.

4.3 | Final remarks and conclusions

Our study provided new insight into the Spanish dehesa functioning and the tree–soil feedback established between crown health, soil functional genes and soil chemistry in soil layers dominated by holm oak roots. This study further showed a potential plant–soil feedback loop in which soil microbiome played a central role determining tree health. The significant adjustments in the functioning of the soil microbial communities at the early stages of tree decline promoted metabolic paths responsible for losing key soil nutrients for tree consumption. This could further result in a loss of dominance of oak trees in declining areas (Gómez-Aparicio et al., 2017). Although numerous studies focus on the unidirectionality of this process (either plant affecting soil or vice versa), we here described the bi-directionality of the causal–effect plant–soil relations as a more plausible way to explain the observed trends of holm oak decline. Factors that affect one component of the feedback (plant or soil) will inexorably affect the other and will potentially boost holm oak decline. Since dehesas are human-shaped ecosystems, it is likely that the process begins with soil disturbance. Identifying the factors that drive this feedback loop, (i.e. loss of nutrients), would be of paramount importance in order to prevent holm oak decline. Land management practices that favour well-drained soils (Ruiz Gómez et al., 2019), transfer soil from healthy trees to affected ones (Bezemer et al., 2020), or promote the inoculation of *Trichoderma* spp and other beneficial microbes (Ruiz-Gómez et al., 2019) can potentially reduce the presence of predisposing factors such as *Phytophthora* spp and thereby break down this declining feedback loop.

AUTHOR CONTRIBUTIONS

Jorge Curiel Yuste and Raquel Esteban were involved in research design. Manuel Encinas-Valero, Jorge Curiel Yuste, Raquel Esteban, Ana-Maria Hereş, María Vivas, Alejandro Solla and Gerardo Moreno were involved in research performance and field sampling. Manuel Encinas-Valero and Raquel Esteban were involved in analytical measurements. Manuel Encinas-Valero, Jorge Curiel Yuste, Raquel Esteban, Lur Epelde and Carlos Garbisu were involved in data analyses. Manuel Encinas-Valero, Jorge Curiel Yuste, Raquel Esteban,

Lur Epelde and Carlos Garbisu were involved in data interpretation. Manuel Encinas-Valero, Jorge Curiel Yuste, Raquel Esteban and Ana-Maria Hereş were involved in manuscript writing. Manuel Encinas-Valero, Jorge Curiel Yuste, Raquel Esteban, Ana-Maria Hereş, María Vivas, Alejandro Solla, Gerardo Moreno, Tamara Corcobado, Iñaki Odriozola, Carlos Garbisu and Lur Epelde were involved in final writing and revision. All authors contributed critically to the drafts and gave final approval for publication.

ACKNOWLEDGEMENTS

This research has been mainly funded by the Spanish Government through the IBERYCA project (CGL2017-84723-P), its associated FPI scholarship BES-2014-067971 (ME-V), the SMARTSOIL (PID2020-113244GB-C21) and SMARTHEALTH (PID2020-113244GA-C22) projects (both funded by MCIN/AEI/10.13039/501100011033). It has been further supported by the BC3 María de Maeztu excellence accreditation (MDM-2017-0714; the Spanish Government), by the BERC 2018–2021 and by the UPV/EHU-GV IT-1648-22 (from the Basque Government). Additionally, this research was further supported through the grant Holistic management practices, modelling and monitoring for European forest soils—HoliSoils (EU Horizon 2020 Grant Agreement No 101000289) and the 'Juan de la Cierva programme' (MV; IJCI-2017-34640; the Spanish Government). We acknowledge the Nutrilab-URJC (Mostoles, Spain) laboratory services for the soil chemical analyses and SGiker of UPV/EHU (Leioa, Spain) for the technical and staff support for the high-throughput quantitative-PCR analysis. We also thank the private owners of the dehesas for facilitating our access to their properties. We are thankful to Celia López-Carrasco Fernández and the 'Consejería de Agricultura, Medioambiente y Desarrollo rural de la Junta de Castilla-La Mancha' for all the logistical support. The 'Tree' icon by Hey Rabbit illustrator, from thenounproject.com were used to design the Graphical abstract. Open Access funding provided by the University of Basque Country.

CONFLICT OF INTEREST STATEMENT

None of the authors have a conflict of interest.

DATA AVAILABILITY STATEMENT

Data deposited in the Dryad Digital Repository: <https://doi.org/10.5061/dryad.gb5mkkwws>, (Encinas-Valero et al., 2023).

ORCID

Manuel Encinas-Valero  <https://orcid.org/0000-0001-9195-283X>

Raquel Esteban  <https://orcid.org/0000-0003-2560-3310>

Ana-Maria Hereş  <https://orcid.org/0000-0002-1839-1770>

María Vivas  <https://orcid.org/0000-0003-2712-417X>

Alejandro Solla  <https://orcid.org/0000-0002-2596-1612>

Gerardo Moreno  <https://orcid.org/0000-0001-8053-2696>

Tamara Corcobado  <https://orcid.org/0000-0001-5762-4728>

Iñaki Odriozola  <https://orcid.org/0000-0002-5289-7935>

Carlos Garbisu  <https://orcid.org/0000-0002-5577-6151>

Lur Epelde  <https://orcid.org/0000-0002-4624-4946>

Jorge Curiel Yuste  <https://orcid.org/0000-0002-3221-6960>

REFERENCES

- Avila, J., Gallardo, A., Ibáñez, B., & Gómez-Aparicio, L. (2016). *Quercus suber* dieback alters soil respiration and nutrient availability in Mediterranean forests. *Journal of Ecology*, *104*, 1441–1452.
- Avila, J. M., Gallardo, A., Ibáñez, B., & Gómez-Aparicio, L. (2021). Pathogen-induced tree mortality modifies key components of the C and N cycles with no changes on microbial functional diversity. *Ecosystems*, *24*, 451–466.
- Avila, M., Gallardo, A., & Gómez-Aparicio, L. (2019). Pathogen-induced tree mortality interacts with predicted climate change to alter soil respiration and nutrient availability in Mediterranean systems. *Biogeochemistry*, *3*, 53–71.
- Barton, K. (2020). *Package 'MuMIn' title multi-model inference*. R package version 1.43.17.
- Bezemer, M., Mangan, S., Reinhart, K., Lance, A. C., Carrino-Kyker, S. R., Burke, D. J., & Burns, J. H. (2020). Individual plant-soil feedback effects influence tree growth and rhizosphere fungal communities in a temperate forest restoration experiment. *Frontiers in Ecology and Evolution*, *1*, 500.
- Bi, Q., Li, K., Zheng, B., Liu, X., & Li, H. (2019). Partial replacement of inorganic phosphorus (P) by organic manure reshapes phosphate mobilizing bacterial community and promotes P bioavailability in a paddy soil. *Science of the Total Environment*, *703*, 134977.
- Boltz, D. F., & Mellon, M. G. (1948). Spectrophotometric determination of phosphorus as molybdiphosphoric acid. *Analytical Chemistry*, *20*, 749–751.
- Camilo-Alves, C. S., da Clara, M., & de Almeida, R. N. (2013). Decline of Mediterranean oak trees and its association with *Phytophthora cinnamomi*: A review. *European Journal of Forest Research*, *132*, 411–432.
- Campbell, B. J., Stein, J. L., & Cary, S. C. (2003). Evidence of chemolithoautotrophy in the bacterial community associated with *Alvinella pompejana*, a hydrothermal vent Polychaete. *Applied and Environmental Microbiology*, *69*, 5070–5078.
- Chen, J., Groenigen, K. v., Hungate, B. A., Terrer, C., Groenigen, J. v., Maestre, F., Ying, S. C., Luo, Y., Jørgensen, U., Sinsabaugh, R. L., Olesen, J., & Elsgaard, L. (2020). Long-term nitrogen loading alleviates phosphorus limitation in terrestrial ecosystems. *Global Change Biology*, *26*, 5077–5086.
- Corcobado, T., Miranda-Torres, J. J., Martín-García, J., Jung, T., & Solla, A. (2017). Early survival of *Quercus ilex* subspecies from different populations after infections and co-infections by multiple *Phytophthora* species. *Plant Pathology*, *66*, 792–804.
- Corcobado, T., Solla, A., Madeira, M. A., & Moreno, G. (2013). Combined effects of soil properties and *Phytophthora cinnamomi* infections on *Quercus ilex* decline. *Plant and Soil*, *373*, 403–413.
- Curiel Yuste, J., Baldocchi, D., Gershenson, A., Goldstein, A., Misson, L., & Wong, S. (2007). Microbial soil respiration and its dependency on carbon inputs, soil temperature and moisture. *Global Change Biology*, *13*, 2018–2035.
- Curiel Yuste, J., Flores-Rentería, D., García-Angulo, D., Hereş, A.-M., Bragă, C., Petritan, A.-M., & Petritan, I. C. (2019). Cascading effects associated with climate-change-induced conifer mortality in mountain temperate forests result in hot-spots of soil CO₂ emissions. *Soil Biology and Biochemistry*, *133*, 50–59.
- Curiel Yuste, J., Ma, S., & Baldocchi, D. D. (2010). Plant-soil interactions and acclimation to temperature of microbial-mediated soil respiration may affect predictions of soil CO₂ efflux. *Biogeochemistry*, *98*, 127–138.
- Deng, L., Peng, C., Kim, D., Li, J., Liu, Y., Hai, X., Liu, Q., Huang, C., Shangquan, Z., & Kuzyakov, Y. (2021). Drought effects on soil carbon and nitrogen dynamics in global natural ecosystems. *Earth-Science Reviews*, *214*, 103501.
- Ehrenfeld, J. G., Ravit, B., & Elgersma, K. (2005). Feedback in the plant-soil system. *Annual Review of Environment and Resources*, *30*, 75–115.
- El-Madany, T. S., Reichstein, M., Carrara, A., Martín, M. P., Moreno, G., Gonzalez-Cascon, R., Peñuelas, J., Ellsworth, D. S., Burchard-Levine, V., Hammer, T. W., Knauer, J., Kolle, O., Luo, Y., Pacheco-Labrador, J., Nelson, J. A., Perez-Priego, O., Rolo, V., Wutzler, T., & Migliavacca, M. (2021). How nitrogen and phosphorus availability change water use efficiency in a Mediterranean savanna ecosystem. *Journal of Geophysical Research: Biogeosciences*, *126*, 1–21.
- Encinas-Valero, M., Esteban, R., Hereş, A.-M., Becerril, J. M., García-Plazaola, J. I., Artexe, U., Vivas, M., Solla, A., Moreno, G., & Curiel, Y. J. (2022). Photoprotective compounds as early markers to predict holm oak crown defoliation in declining Mediterranean savannahs. *Tree Physiology*, *42*, 208–224.
- Encinas-Valero, M., Esteban, R., Heres, A.-M., Vivas, M., Fakhet, D., Aranjuelo, I., Solla, A., Moreno, G., & Curiel Yuste, J. (2022). Holm oak decline is determined by shifts in fine root phenotypic plasticity in response to belowground stress. *New Phytologist*, *235*, 2237–2251.
- Encinas-Valero, M., Esteban, R., Heres, A.-M., Vivas, M., Solla, A., Moreno, G., Corcobado, T., Odriozola, I., Garbisu, C., Epelde, L., & Curiel Yuste, J. (2023). Data from: Biogeochemical cycles in holm oak dehesas. *Dryad Dryad Digital Repository*. <https://doi.org/10.5061/dryad.gb5mkkwvs>
- Esteban, R., Barrutia, O., Artetxe, U., Fernández-Marín, B., Hernández, A., & García-Plazaola, J. I. (2015). Internal and external factors affecting photosynthetic pigment composition in plants: A meta-analytical approach. *New Phytologist*, *206*, 268–280.
- Flores-Rentería, D., Rincón, A., Morán-López, T., Hereş, A.-M., Pérez-Izquierdo, L., Valladares, F., & Curiel Yuste, J. (2018). Habitat fragmentation is linked to cascading effects on soil functioning and CO₂ emissions in Mediterranean holm-oak-forests. *PeerJ*, *6*, e5857.
- Fox, J., & Weisberg, S. (2019). *An R companion to applied regression* (3rd ed.). Sage.
- Francis, C. A., Roberts, K. J., Beman, J. M., Santoro, A. E., & Oakley, B. B. (2005). Ubiquity and diversity of ammonia-oxidizing archaea in water columns and sediments of the ocean. *Proceedings of the National Academy of Sciences of the United States of America*, *102*, 14683–14688.
- García-Angulo, D. (2020). Efectos del decaimiento del encinar Mediterráneo inducido por sequía y del papel modulador del manejo histórico sobre los ciclos biogeoquímicos y las comunidades microbianas del suelo.
- García-Angulo, D., Hereş, A. M., Fernández-López, M., Flores, O., Sanz, M. J., Rey, A., Valladares, F., & Curiel Yuste, J. (2020). Holm oak decline and mortality exacerbates drought effects on soil biogeochemical cycling and soil microbial communities across a climatic gradient. *Soil Biology and Biochemistry*, *149*, 107921.
- García-Plazaola, J. I., Hernández, A., Fernández-Marín, B., Esteban, R., José Peguero-Pina, J. J., Verhoeven, A., & Cavender-Bares, J. (2017). Photoprotective mechanisms in the genus *Quercus* in response to winter cold and summer drought. In E. Gil-Pelegrín, J. J. Peguero-Pina, & D. Sancho-Knapik (Eds.), *Oaks physiological ecology. Exploring the functional diversity of genus Quercus L* (pp. 361–393). Springer International Publishing.
- Gea-Izquierdo, G., Natalini, F., & Cardillo, E. (2021). Holm oak death is accelerated but not sudden and expresses drought legacies. *Science of the Total Environment*, *754*, 141793.
- Gómez-Aparicio, L., Domínguez-Begines, J., Kardol, P., Ávila, J. M., Gomez-aparicio, L., Dominguez-begines, J., Kardol, P., Avila, J. M., Ibáñez, B., & Garcia, L. V. (2017). Plant-soil feedbacks in declining forests: Implications for species coexistence. *Ecology*, *98*, 1908–1921.
- Harrell, F. (2019). *Hmisc: Harrell miscellaneous*. R package version 4.3.0.
- Harris, I., Osborn, T. J., Jones, P., & Lister, D. (2020). Version 4 of the CRU TS monthly high-resolution gridded multivariate climate dataset. *Scientific Data*, *7*, 1–18.

- Harris, J., & Bedfordshire, M. K. (2003). Measurements of the soil microbial community for estimating the success of restoration. *European Journal of Soil Science*, *54*, 801–808.
- Henry, S., Bru, D., Stres, B., Hallet, S., Philippot, L., & Al, H. E. T. (2006). Quantitative detection of the *nosZ* gene, encoding nitrous oxide reductase, and comparison of the abundances of 16S rRNA, *narG*, *nirK*, and *nosZ* genes in soils. *Applied and Environmental Microbiology*, *72*, 5181–5189.
- Hwangbo, H., Park, R. D., Kim, Y. W., Rim, Y. S., Park, K. H., Kim, T. H., Suh, J. S., & Kim, K. Y. (2003). 2-Ketogluconic acid production and phosphate solubilization by *Enterobacter* intermedium. *Current Microbiology*, *47*, 87–92.
- Ibañez, M., Chocarro, C., Aljazairi, S., Ribas, À., & Sebasti, M. (2021). Tree-open grassland structure and composition drive greenhouse gas exchange in holm oak meadows of the Iberian peninsula. *Agronomy*, *11*, 1–16.
- Juvany, M., Müller, M., & Munné-Bosch, S. (2013). Photo-oxidative stress in emerging and senescing leaves: A mirror image? *Journal of Experimental Botany*, *64*, 3087–3098.
- Kalra, Y. P. (1995). Determination of pH of soils by different methods: Collaborative study. *Journal of AOAC International*, *78*, 310–324.
- Kowalchuk, G. A., Buma, D. S., De Boer, W., Klinkhamer, P. G. L., & Van Veen, J. A. (2002). Effects of above-ground plant species composition and diversity on the diversity of soil-borne microorganisms. *Antonie Van Leeuwenhoek*, *81*, 509–520.
- Krom, M. D. (1980). Spectrophotometric determination of ammonia: A study of a modified berthelot reaction using salicylate and dichloroisocyanurate. *The Analyst*, *105*, 305–316.
- Lefcheck, J. S. (2016). piecewiseSEM: Piecewise structural equation modelling in R for ecology, evolution, and systematics. *Methods in Ecology and Evolution*, *7*, 573–579.
- Lennon, E. F. E., & Houlton, B. Z. (2017). Coupled molecular and isotopic evidence for denitrifier controls over terrestrial nitrogen availability. *The ISME Journal*, *11*, 727–740.
- Lenth, R. (2020). *emmeans: Estimated marginal means, aka least-squares means*. R package version 1.4.6.
- Levy-Booth, D. J., Prescott, C. E., & Grayston, S. J. (2014). Microbial functional genes involved in nitrogen fixation, nitrification and denitrification in forest ecosystems. *Soil Biology and Biochemistry*, *75*, 11–25.
- Looft, T., Johnson, T. A., Allen, H. K., Bayles, D. O., Alt, D. P., Stedtfield, R. D., Sul, W. J., Stedtfield, T. M., Chai, B., Cole, J. R., Hashsham, S. A., Tiedje, J. M., & Stanton, T. B. (2012). In-feed antibiotic effects on the swine intestinal microbiome. *Proceedings of the National Academy of Sciences of the United States of America*, *109*, 1691–1696.
- López-Sánchez, A., Capó, M., Rodríguez-Calcerrada, J., Solla, A., Martín, J. A., & Perea, R. (2022). Exploring the use of solid biofertilisers to mitigate the effects of exploring the use of solid biofertilisers to mitigate the effects of *Phytophthora* oak root disease. *Forests*, *13*(10), 1558.
- Margalef, O., Sardans, J., & Janssens, I. A. (2017). Global patterns of phosphatase activity in natural soils. *Scientific Reports*, *7*, 1–13.
- Marklein, A. R., & Houlton, B. Z. (2012). Nitrogen inputs accelerate phosphorus cycling rates across a wide variety of terrestrial ecosystems. *New Phytologist*, *193*, 696–704.
- Meng, S., Peng, T., Liu, X., Wang, H., Huang, T., Gu, J., & Hu, Z. (2022). *Ecological role of bacteria involved in the biogeochemical cycles of mangroves based on functional genes detected through GeoChip 5.0* (p. 7). American Society for Microbiology.
- Meyer, G., Maurhofer, M., Frossard, E., Gamper, H. A., Mäder, P., Mészáros, É., Schönholzer-Mauclair, L., Symanczik, S., & Oberson, A. (2019). *Pseudomonas protegens* CHAO does not increase phosphorus uptake from ³²P labeled synthetic hydroxyapatite by wheat grown on calcareous soil. *Soil Biology and Biochemistry*, *131*, 217–228.
- Moreno, G., Obrador, J., García, E., Cubera, E., Montero, M. J., Pulido, F., & Dupraz, C. (2007). Driving competitive and facilitative interactions in oak dehesas through management practices. *Agroforestry in Europe*, *70*, 25–40.
- Moreno, G., Obrador, J. J., Cubera, E., & Dupraz, C. (2005). Fine root distribution in dehesas of Central-Western Spain. *Plant and Soil*, *277*, 153–162.
- Moreno, G., & Pulido, F. (2009). The functioning, management and persistence of dehesas. In A. Rigueiro-Rodríguez & M. A. JM-LM (Eds.), *Agroforestry in Europe*. Advances in Agroforestry (Vol. 6). Springer.
- Navone, R. (1964). Proposed method for nitrate in potable waters. *Journal-American Water Works Association*, *56*, 781–783.
- Oksanen, J., Simpson, G., Blanchet, F., Kindt, R., Legendre, P., Minchin, P., O'Hara, R., Solymos, P., Stevens, M., Szoecs, E., Wagner, H., Barbour, M., Bedward, M., Bolker, B., Borcard, D., Carvalho, G., Chirico, M., De Caceres, M., Durand, S., ... Weedon, J. (2022). *_vegan: Community ecology package_*. R package version 2.6-4. <https://CRAN.R-project.org/package=vegan>
- Pinho, D., Barroso, C., Froufe, H., Brown, N., Vanguelova, E., & Denman, S. (2020). Linking tree health, rhizosphere physicochemical properties, and microbiome in acute oak decline. *Forests*, *11*(11), 1153.
- Png, G. K., De Long, J. R., Fry, E. L., Heinen, R., Heinze, J., Morriën, E., Sapsford, S. J., & Teste, F. P. (2023). Plant-soil feedback: The next generation. *Plant and Soil*, *485*, 1–5.
- Prescott, C. E. (2002). The influence of the forest canopy on nutrient cycling. *Tree Physiology*, *22*, 1193–1200.
- Pulido, F., Díaz, M., & Sebastian, J. (2001). Size structure and regeneration of Spanish holm oak *Quercus ilex* forests and dehesas: Effects of agroforestry use on their long-term sustainability. *Forest Ecology and Management*, *146*, 1–13.
- R Core Team. (2020). *A language and environment for statistical computing*. R Foundation for Statistical Computing. R (v. 4.0.0, 2020).
- Radojevic, M., Bashkin, V., & Bashkin, V. (1999). *Practical environmental analysis*. Royal Society of Chemistry.
- Ragot, S., Kertesz, M., Meszaros, E., Frossard, E., & Bunemann, E. (2017). Soil *phoD* and *phoX* alkaline phosphatase gene. *FEMS Microbiology Ecology*, *93*, 1–15.
- Rasche, F., Knapp, D., Kaiser, C., Koranda, M., Kitzler, B., Zechmeister-boltenstern, S., Richter, A., & Sessitsch, A. (2011). Seasonality and resource availability control bacterial and archaeal communities in soils of a temperate beech forest. *The ISME Journal*, *5*, 389–402.
- Raymond, N. S., Raymond, N. S., Beatriz, G., Nybroe, O., Jensen, L. S., Dorette, S. M., & Richardson, A. E. (2020). Phosphate-solubilising microorganisms for improved crop productivity: A critical assessment. *New Phytologist*, *229*, 1268–1277.
- Refsland, T. K., Adams, B., Bronson, D., Kern, C. C., Marquardt, P., McGraw, A. M., Royo, A. A., & Miesel, J. R. (2023). Synthesis of plant-soil feedback effects on eastern North American tree species: Implications for climate-adaptive forestry. *Frontiers in Ecology and Evolution*, *11*, 1073724.
- Richards, L. A. (1954). Diagnosis and improvement of saline and alkali soils. *The Hand*, *78*, 154.
- Rodríguez, A., Curiel Yuste, J., Rey, A., Durán, J., García-Camacho, R., Gallardo, A., & Valladares, F. (2016). Holm oak decline triggers changes in plant succession and microbial communities, with implications for ecosystem C and N cycling. *Plant and Soil*, *414*, 247–263.
- Rodríguez, A., Durán, J., Rey, A., Boudouris, I., Valladares, F., Gallardo, A., & Yuste, J. C. (2019). Interactive effects of forest die-off and drying-rewetting cycles on C and N mineralization. *Geoderma*, *333*, 81–89.
- Rodríguez, A., Durán, J., Yuste, J. C., Valladares, F., & Rey, A. (2023). The effect of tree decline over soil water content largely controls soil respiration dynamics in a Mediterranean woodland. *Agricultural and Forest Meteorology*, *333*, 109398.
- Rodríguez-Calcerrada, J., Sancho-Knapik, D., Martin-StPaul, N. K., Limousin, J.-M., McDowell, N. G., & Gil-Pelegrín, E. (2017).

- Drought-induced oak decline-factors involved, physiological dysfunctions and potential attenuation by forestry practises. In E. Gil-Pelegrín, J. Peguero-Pina, & D. Sancho-Knapik (Eds.), *Oaks physiological ecology. Exploring the functional diversity of genus Quercus. Tree Physiology*, 7. Springer.
- Rösch, C., & Bothe, H. (2005). Improved assessment of denitrifying, N₂-fixing, and total-community bacteria by terminal restriction fragment length polymorphism analysis using multiple restriction enzymes. *Applied and Environmental Microbiology*, 71, 2026–2035.
- Ruiz Gómez, F. J., Navarro-Cerrillo, R. M., Pérez-de-Luque, A., Oßwald, W., Vannini, A., & Morales-Rodríguez, C. (2019). Assessment of functional and structural changes of soil fungal and oomycete communities in holm oak declined dehesas through metabarcoding analysis. *Scientific Reports*, 9(1), 5315.
- Ruiz-Gómez, F. J., Pérez-de-Luque, A., & Navarro-Cerrillo, R. M. (2019). The involvement of phytophthora root rot and drought stress in holm oak decline: From ecophysiology to microbiome influence. *Current Forestry Reports*, 5, 251–266.
- Sánchez-Cuesta, R., González-Moreno, P., Cortés-Márquez, A., Navarro-Cerrillo, R. M., & Ruiz-Gómez, F. J. (2022). Soil distribution of *Phytophthora cinnamomi* inoculum in oak afforestation depends on site characteristics rather than host availability. *New Forests*, 54, 1–23.
- Sánchez-Cuesta, R., Ruiz-Gómez, F. J., Duque-Lazo, J., González-Moreno, P., & Navarro-Cerrillo, R. M. (2021). The environmental drivers influencing spatio-temporal dynamics of oak defoliation and mortality in dehesas of Southern Spain. *Forest Ecology and Management*, 485, 118946.
- San-Emeterio, L. M., Jiménez-morillo, N. T., & Pérez-ramos, I. M. (2023). Changes in soil organic matter molecular structure after five years mimicking climate change scenarios in a Mediterranean savannah. *Science of the Total Environment*, 857, 159288.
- Sardans, J., Rodà, F., & Peñuelas, J. (2004). Phosphorus limitation and competitive capacities of *Pinus halepensis* and *Quercus ilex* subsp. *rotundifolia* on different soils. *Plant Ecology*, 174, 305–317.
- Scarlett, K., Denman, S., Clark, D. R., Forster, J., Vanguelova, E., Brown, N., & Whitby, C. (2020). Relationships between nitrogen cycling microbial community abundance and composition reveal the indirect effect of soil pH on oak decline. *The ISME Journal*, 15(3), 1–13.
- Searle, P. L. (1984). The Berthelot or Indophenol reaction and its use in the analytical chemistry of nitrogen. A review. *Analyst*, 109, 549–568.
- Serrano, M. S., Fernández-Rebollo, P., De Vita, P., & Sánchez, M. E. (2013). Calcium mineral nutrition increases the tolerance of *Quercus ilex* to *Phytophthora* root disease affecting oak rangeland ecosystems in Spain. *Agroforestry Systems*, 87, 173–179.
- Shvaleva, A., Siljanen, H., Correia, A., Silva, F., Lamprecht, R., Lobo-Vale, R., Bicho, C., Fangueiro, D., Anderson, M., Pereira, J. S., Chaves, M. M., Cruz, C., & Martikainen, P. J. (2015). Environmental and microbial factors influencing methane and nitrous oxide fluxes in Mediterranean cork oak woodlands: Trees make a difference. *Frontiers in Microbiology*, 6, 1104.
- Singh, A., Kumar, M., & Saxena, A. K. (2020). Role of microorganisms in regulating carbon cycle in tropical and subtropical soils. In P. Ghosh, D. Mandal, S. Ramakrishnam, S. Mahanta, & B. Mandal (Eds.), *Carbon management in tropical and sub-tropical terrestrial systems*. Springer.
- Smith, P., Cotrufo, M. F., Rumpel, C., Paustian, K., Kuikman, P. J., Elliott, J. A., McDowell, R., Griffiths, R. I., Asakawa, S., Bustamante, M., House, J. I., Sobocká, J., Harper, R., Pan, G., West, P. C., Gerber, J. S., Clark, J. M., Adhya, T., Scholes, R. J., & Scholes, M. C. (2015). Biogeochemical cycles and biodiversity as key drivers of ecosystem services provided by soils. *The Soil*, 1, 665–685.
- Solís-García, I., Ceballos-Luna, O., Cortazar-Murillo, E. M., Desgarenes, D., Edith, G.-S., Patiño-Conde, V., Guevara-Avenida, E., Méndez-Bravo, A., & Reverchon, F. (2021). *Phytophthora* root rot modifies the composition of the avocado rhizosphere microbiome and increases the abundance of opportunistic fungal pathogens. *Frontiers in Microbiology*, 11, 1–15.
- Solla, A., Moreno, G., Malewski, T., Jung, T., Klisz, M., Tkaczyk, M., Siebyla, M., Pérez, A., Cubera, E., Hrynyk, H., Szulc, W., Rutkowska, B., Martín, J. A., Belbahri, L., & Oszak, T. (2021). Phosphite spray for the control of oak decline induced by *Phytophthora* in Europe. *Forest Ecology and Management*, 485, 118938.
- Strasser, R. J., Srivastava, A., & Tsimilli-Michael, M. (2000). The fluorescence transient as a tool to characterize and screen photosynthetic samples. *Probing Photosynthesis: Mechanism, Regulation & Adaptation*, 25, 443–480.
- Tu, Q., Yu, H., He, Z., Deng, Y., Wu, L., Nostrand, J., Shi, Z., Xue, K., Yuan, T., Wang, A., & Zhou, J. (2014). GeoChip 4: A functional gene-array-based high-throughput environmental technology for microbial community analysis. *Molecular Ecology Resources*, 14, 914–928.
- van der Putten, W. H., Bradford, M. A., Pernilla Brinkman, E., van de Voorde, T. F. J., & Veen, G. F. (2016). Where, when and how plant-soil feedback matters in a changing world. *Functional Ecology*, 30, 1109–1121.
- Venables, W. N., & Ripley, B. D. (2002). *Modern applied statistics with S* (4th ed.). Springer. ISBN 0-387-95457-0.
- Walinga, I., Van Der Lee, J. J., Houba, V. J. G., Van Vark, W., & Van Der Lee, J. J. (1989). Part 7. In *Plant analysis procedure* (pp. 197–200). Syllabus.
- Wei, W., Isobe, K., Nishizawa, T., Zhu, L., Shiratori, Y., Ohte, N., Koba, K., Otsuka, S., & Senoo, K. (2015). Higher diversity and abundance of denitrifying microorganisms in environments than considered previously. *The ISME Journal*, 9, 1954–1965.
- Willey JM, Sherwood LM, Woolverton C. 2008. *Prescott, Harley, and Klein's microbiology*. McGraw-Hill.
- Wu, X., Rensing, C., Han, D., Xiao, K., Dai, Y., Tang, Z., & Liesack, W. (2022). Genome-resolved metagenomics reveals distinct phosphorus acquisition strategies between soil microbiomes. *American Society for Microbiology*, 7(1), e01107-21.
- Xiao, H., Xiao, Y., Xu, M., Wang, Z., Wang, L., Wang, J., & Shi, Z. (2022). Role of autotrophic microbes in organic matter accumulation in soils degraded by erosion. *Land Degradation and Development*, 33, 2092–2102.
- Yeomans, J. C., & Bremner, J. M. (1988). A rapid and precise method for routine determination of organic carbon in soil. *Communications in Soil Science and Plant Analysis*, 19, 1467–1476.
- Zheng, B., Zhu, Y., Sardans, J., Peñuelas, J., & Su, Q. (2018). QMEC: A tool for high-throughput quantitative assessment of microbial functional potential in C, N, P, and S biogeochemical cycling key. *Science China*, 61, 1451–1462.

SUPPORTING INFORMATION

Additional supporting information can be found online in the Supporting Information section at the end of this article.

Table S1. Mean and standard error of the defoliation and the early stress markers (i.e. photosynthetic performance index, chlorophylls, VAZ and total tocopherol) for each health status: healthy, susceptible and declining.

Table S2. Abbreviation of the soil microbial functional gene and encoded enzyme used in this study.

Table S3. Species-specific primers used in this study to detect the presence of *Phytophthora* spp-induced holm oak decline.

Table S4. Results of the first set of linear mixed-effect models (LMEs) that show the relative abundance of the soil microbial functional genes as a function of the health status (i.e. healthy, susceptible and declining).

Table S5. Results of the linear mixed-effect models (LMEs) in which the functional-gene relative abundance of the different biogeochemical cycles: carbon cycling (carbon hydrolysis, carbon fixation, methane metabolism), phosphorus cycling, nitrogen cycling and sulfur cycling were fitted as a function of belowground and aboveground tree compartment.

Figure S1. Panel A; Depiction of the land use and management of the studied dehesas.

Figure S2. Heatmap analyses of gen abundance relative to the 16S rRNA gene.

Figure S3. Scatter plot showing the change in the soil chemical

properties of the susceptible and declining holm oak trees relative to the healthy holm oak trees.

How to cite this article: Encinas-Valero, M., Esteban, R., Hereş, A.-M., Vivas, M., Solla, A., Moreno, G., Corcobado, T., Odriozola, I., Garbisu, C., Epelde, L., & Curiel Yuste, J. (2023). Alteration of the tree–soil microbial system triggers a feedback loop that boosts holm oak decline. *Functional Ecology*, 00, 1–17. <https://doi.org/10.1111/1365-2435.14473>